

Synthesis and Evaluation of Biological Activities for a Novel 1,2,3,4-Tetrahydroisoquinoline Conjugate with Dipeptide Derivatives: Insights from Molecular Docking and Molecular Dynamics Simulations

Sunil R. Tivari,[¶] Siddhant V. Kokate,[¶] José L. Belmonte-Vázquez, Tushar Janardan Pawar, Harun Patel, Iqrar Ahmad, Manoj S. Gayke, Rajesh S. Bhosale, Vicky D. Jain, Ghazala Muteeb,* Enrique Delgado-Alvarado,* and Yashwantsinh Jadeja*



Cite This: *ACS Omega* 2023, 8, 48843–48854



Read Online

ACCESS |



Metrics & More

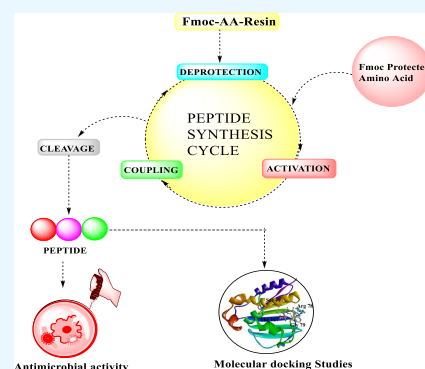


Article Recommendations



Supporting Information

ABSTRACT: Peptide synthesis has opened new frontiers in the quest for bioactive molecules with limitless biological applications. This study presents the synthesis of a series of novel isoquinoline dipeptides using advanced spectroscopic techniques for characterization. These compounds were designed with the goal of discovering unexplored biological activities that could contribute to the development of novel pharmaceuticals. We evaluated the biological activities of novel compounds including their antimicrobial, antibacterial, and antifungal properties. The results show promising activity against *Escherichia coli* and potent antibacterial activity against MTCC 443 and MTCC 1688. Furthermore, these compounds demonstrate strong antifungal activity, outperforming existing standard drugs. Computational binding affinity studies of tetrahydroisoquinoline-conjugated dipeptides against *E. coli* DNA gyrase displayed significant binding interactions and binding affinity, which are reflected in antimicrobial activities of compounds. Our integrative significant molecular findings from both wet and dry laboratories would help pave a path for the development of antimicrobial therapeutics. The findings suggest that these isoquinoline-conjugated dipeptides could be excellent candidates for drug development, with potential applications in the fight against bacterial and fungal infections. This research represents an exciting step forward in the field of peptide synthesis and its potential to discover novel bioactive molecules with significant implications for human health.



INTRODUCTION

Drug-resistant infections have become a growing public health concern, with an increasing number of pathogens developing resistance to commonly used antibiotics.^{1–3} This has led to an urgent need for the development of new and effective antimicrobial agents to combat these infections. The emergence of multidrug-resistant bacterial strains has been linked to the overuse and misuse of antibiotics, leading to the selection of resistant strains.⁴ In addition, the development of new antibiotics has been slow and relatively few new antibiotics are currently in development.⁵ Therefore, the need for new antimicrobial agents to address drug-resistant infections is pressing.

Antimicrobial peptides (AMPs) have emerged as a promising class of molecules that can be used to address this problem.^{6,7} These peptides have a broad spectrum of activity against bacteria, fungi, and viruses and are less likely to develop resistance compared to conventional antibiotics.^{8–10} AMPs are produced by various organisms, including plants, animals, and microorganisms, and they play a vital role in the innate immune system's defense against pathogens.^{11–13} These

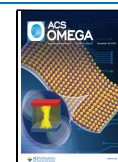
peptides are typically small and cationic, allowing them to interact with microorganisms' negatively charged cell membranes, leading to membrane disruption and cell death.^{14,15} Over the past few decades, there have been substantial progress in the field of AMPs, with an increasing number of these peptides being discovered and characterized.^{16–19} These developments have revolutionized the medicinal field, providing new hope in the fight against drug-resistant infections. The discovery of AMPs has led to the development of various peptide-based drugs with significant potential in the pharmaceutical industry.²⁰ These peptides have shown promising activity against bacterial and fungal infections and various viral infections as well, including HIV.^{21,22}

Received: August 24, 2023

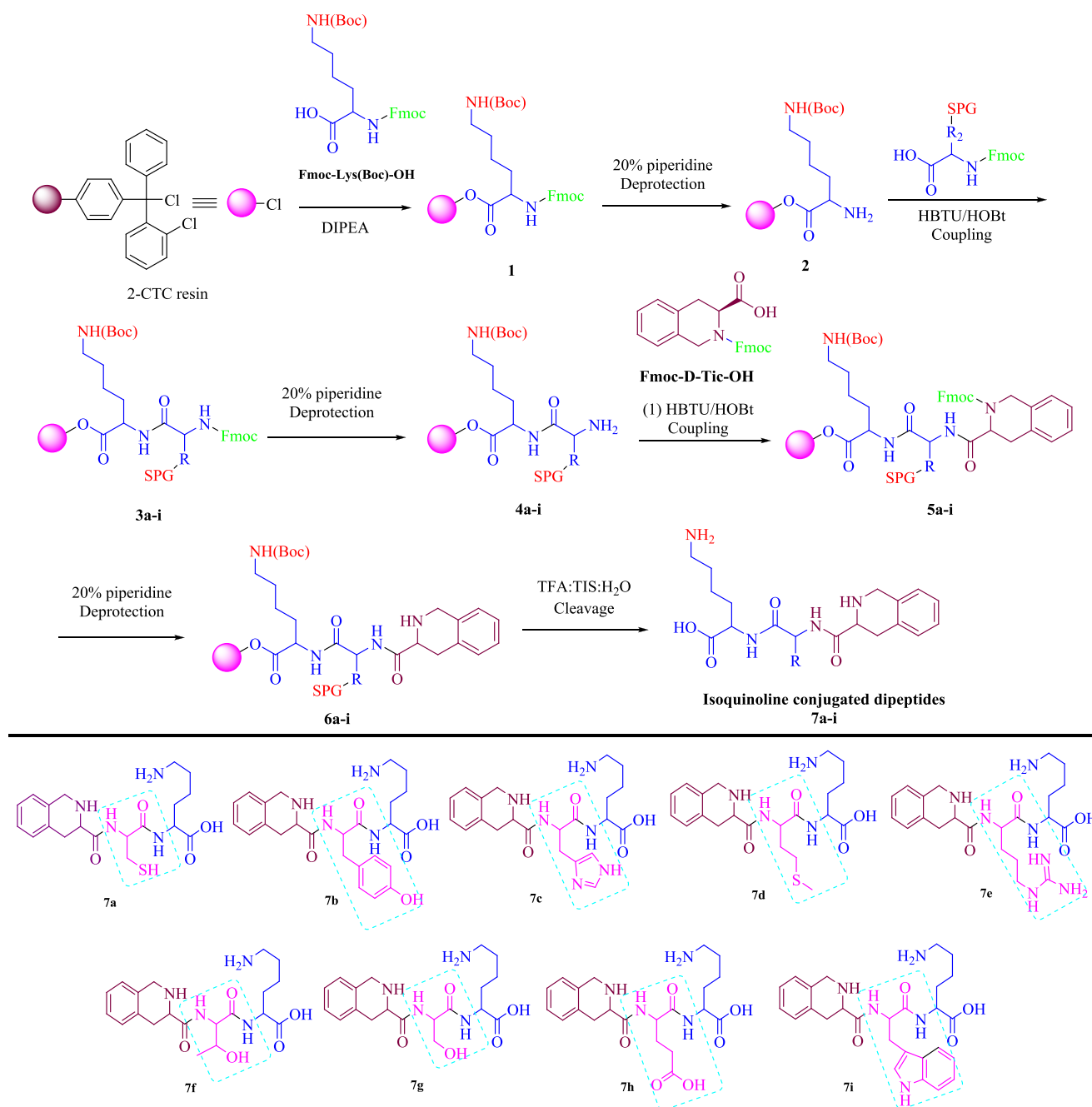
Revised: November 24, 2023

Accepted: November 28, 2023

Published: December 12, 2023



Scheme 1. Synthetic Route for the Preparation of Title Compounds 7a–i



Cationic peptides are a subcategory of AMPs that are characterized by their positively charged amino acid residues, such as histidine (His), lysine (Lys), or arginine (Arg).²³ The cationic nature of these peptides plays a crucial role in their antimicrobial activity, as it allows them to interact with the negatively charged cell membrane of a bacteria and disrupt its integrity.^{24,25} Furthermore, cationic peptides have been shown to possess immunomodulatory properties, promoting wound healing and reducing inflammation.²⁶

Global researchers are actively engaged in the exploration and synthesis of innovative therapeutic compounds incorporating heterocyclic scaffolds. This interest stems from the ubiquitous presence of heterocyclic structures in nature, their diverse synthetic applications, and their wide array of biological activities.^{27–31} Nitrogen-containing heterocycles, in particular,

have garnered significant attention due to their superior biological applicability compared to their oxygen and sulfur counterparts.^{32–34} Among these nitrogen-containing heterocycles, 1,2,3,4-tetrahydroisoquinoline (THIQ), an aromatic heterocyclic compound featuring a nitrogen atom, holds paramount importance for medicinal chemists seeking to develop novel and potent therapeutics. THIQ derivatives exhibit notable biological activities, including but not limited to anticancer,³⁵ antitubercular,³⁶ antibacterial,³⁷ antifungal,³⁸ anti-HIV,³⁹ and anti-inflammatory,⁴⁰ properties. Consequently, THIQ represents a crucial and extensively utilized member of the heterocyclic compound family. Notably, numerous pharmaceutical products in the market incorporate THIQ moieties, such as quinapril,⁴¹ noscapine,⁴² tubocurari,⁴³ and apomorphine.⁴⁴

Globally, researchers widely prefer the solid support approach (solid-phase peptide synthesis or SPPS) over the liquid phase technique (liquid-phase peptide synthesis or LPPS) for the synthesis of AMPs, especially for longer peptide sequences. SPPS, known for its efficiency, employs straightforward synthetic processes and simple purification methods, enabling the rapid synthesis of linear peptides with high purity. Unlike LPPS, SPPS eliminates the need for isolating intermediates or time-consuming procedures, making it a more effective option. Its applicability extends to the synthesis of peptides with varying complexities, including short or long chains as well as cyclic structures. Notably, SPPS protocols can be fully automated and the utilization of automated peptide synthesizers significantly enhances its scalability.⁴⁵

In light of these facts, we designed and synthesized a novel class of short dipeptide-heterocycle hybrids **7a–i**, comprising a THIQ-3-carboxylic acid constituent at the N-terminus and lysine at the C-terminus, by utilizing the SPPS protocol (Scheme 1). The dipeptides were synthesized using lysine as the amino acid to introduce cationic properties to the peptides.²³ The cationic nature of these peptides allows them to interact with the negatively charged bacterial cell membrane and disrupt its integrity, thus playing a crucial role in their antimicrobial activity. Therefore, we have designed our synthetic protocol solely based on the fact that having a cationic amino acid, like Lys in our sequence, will enhance the positive charge on the overall molecule, which in turn will enhance its biological activity. Lys was constant in all peptides, and the second AA was changed. The other two cationic AAs, Arg and His, were incorporated with the anticipation that those THIQ peptides will give good biological activity due to their cationic behavior. Moreover, we have used AAs with polar uncharged side chains, such as serine (Ser) and threonine (Thr), and AAs with hydrophobic side chains, such as tyrosine (Tyr), methionine (Met), and tryptophan (Trp), to show the effect of side chains on the biological activities of the synthesized compounds. Furthermore, we assessed the antimicrobial efficacy of the resulting hybrids, comparing their activities to those of the standard antibacterial drug ampicillin and the standard antifungal drug nystatin. Additionally, we conducted *in silico* studies on the synthesized short peptide derivatives. The synthesis methodology facilitated easy purification steps, eliminating the need for the isolation of intermediate products during the dipeptide synthesis. The comprehensive approach, combining experimental and *in silico* investigations of the prepared derivatives **7a–i**, holds promise in establishing safe and efficient therapeutics to combat antimicrobial resistance (AMR).

RESULTS AND DISCUSSION

A series of experiments were conducted to create a novel class of peptide-heterocycle hybrids known as THIQ-3-carboxylic acid constituents conjugated with short dipeptide motifs **7a–i**. The methodology employed for their synthesis, namely, the solid-phase peptide synthesis (SPPS) approach using the HBTU/HOBt condensation protocol, was carefully selected to ensure the highest possible yield. Yields of all the synthesized derivatives were in the range of 78–89%. Notably, the resulting peptide derivatives were obtained in a remarkably stable solid powder form, underscoring the reliability and robustness of the synthesis process. We have used similar synthetic procedures for the synthesis of desired products that we have used in our previously reported work.³¹

Delving deeper into the intricacies of the synthesis process, the construction of dipeptide derivatives containing THIQ moiety **7a–i** was meticulously illustrated through a comprehensive step-by-step description outlined in Scheme 1. This synthetic pathway involved a series of precisely controlled chemical reactions, including condensation and deprotection steps, all carefully orchestrated to achieve the desired molecular structure. A critical aspect of the synthesis involved the attachment of the first amino acid (AA), which is Fmoc-Lys(Boc)-OH, utilizing DIPEA in DCM to afford Fmoc-Lys(Boc)-2-CTC resin **1**, which is a fundamental building block for the subsequent steps. The successful formation of this compound was pivotal and served as the basis for the subsequent stages of the synthesis process. To carry out the condensation of further AAs, deprotection of the Fmoc group of **1** was necessary, which was carried out using 20% piperidine/DMF. The Fmoc group removal afforded NH₂-Lys(Boc)-2-CTC resin **2**, consisting of the free amino (–NH₂) group at the N-terminal. The completion of Fmoc deprotection was ensured by performing the Kaiser test. The blue color resin beads and Kaiser test solution confirmed the Fmoc removal completion. Furthermore, the condensation reaction condition utilizing HBTU/DIPEA/HOBt combination was employed for the condensation of next Fmoc-AAs, Fmoc-R(SPG)-OH, where R is a different AA and SPG is a side-chain-protecting group. Again, the Kaiser test was carried out to check the completion of the condensation step. The obtained colorless resin beads and test solution indicated the completion of condensation reaction. The intermediates **3a–i** and **4a–i** were synthesized by using similar cycles of deprotection and condensation steps.

Furthermore, condensation of **4a–i** with Fmoc-D-Tic-OH (*N*-1-Fmoc-D-1,2,3,4-tetrahydro-isoquinoline-3-carboxylic acid) by employing the aforementioned HBTU/DIPEA/HOBt condensation reaction condition yielded different D-Tic-R(SPG)-Lys(Boc)-2-CTC resin derivatives **5a–i**. The Fmoc group of **5a–i** was deprotected by using 20% piperidine in DMF to yield **6a–i**. Finally, the global cleavage, acidolysis, of **6a–i** was carried out to cleave the CTC resin and all SPGs from the desired peptide chain using the cleavage cocktail of TFA:H₂O:TIS in a ratio 80:10:10. The precipitation was carried out using DIPE to afford the desired THIQ-conjugated dipeptides. Ethyl acetate and *n*-hexanes were utilized for further purification of crude products and yielded pure desired derivatives **7a–i** in 78–89% yields. The advantage of carrying out the SPPS of the desired THIQ-conjugated dipeptides was that all of the condensation reactions were carried out *in situ* and no isolation of intermediates was needed. Each intermediate product was rigorously tested and validated through the Kaiser test, ensuring the purity and integrity of the chemical transformations at every step. The strategic incorporation of various Fmoc-protected AAs and different SPGs at specific stages of the synthesis process facilitated the production of a diverse set of compounds, each possessing unique structural characteristics. These variations in the molecular composition of the peptides, such as the inclusion of cationic, polar, negative, and hydrophobic substitutions, were essential for the comprehensive evaluation of the bioactive properties of the synthesized compounds.

The structures of **7a–i** were characterized using ¹H, ¹³C NMR, and mass spectral analyses (Figures S9–S34). All the spectral data confirm the structures of desired THIQ-conjugated **7a–i** compounds. In ¹³C NMR, it was observed

Table 1. Antibacterial and Antifungal Activities of Synthesized Compounds 7a–i

entry	name of compounds	MIC (antibacterial activity) in μM				MIC (antifungicidal activity) in μM	
		<i>E. c.</i>	<i>P. a.</i>	<i>S. a.</i>	<i>S. p.</i>	<i>C. a.</i>	<i>A. n.</i>
7a	D-Tic-Cys-Lys-OH	415	498	664	830	664	664
7b	D-Tic-Tyr-Lys-OH	166	166	830	1661	332	664
7c	D-Tic-His-Lys-OH	33	166	498	332	166	265
7d	D-Tic-Met-Lys-OH	498	332	664	498	415	365
7e	D-Tic-Arg-Lys-OH	166	83	830	315	166	332
7f	D-Tic-Thr-Lys-OH	498	664	830	830	830	1661
7g	D-Tic-Ser-Lys-OH	66	332	664	415	265	166
7h	D-Tic-Glu-Lys-OH	166	332	830	747	332	1661
7i	D-Tic-Trp-Lys-OH	332	332	664	764	332	664
Std1	ampicillin	332	332	830	332		
Std2	nystatin					332	332

that spectra of all the compounds have extra signals at 115–120 and 60 ppm apart from the desired signals. In all the compounds, the Lys moiety forms the TFA salt giving rise to those additional signals of TFA in ^{13}C NMR. In synthesized series of peptides, we used different amino acid substitutions, including cationic substitutions in peptides 7c (His) and 7e (Arg), polar substitutions in peptides 7f (Thr) and 7g (Ser), negative substitution in peptide 7h (Glu), and a special case of amino acid substitution in peptide 7a (Cys). In addition, hydrophobic substitutions were also explored in peptides 7b (Tyr), 7d (Met), and 7i (Trp) to evaluate their bioactivities. Overall, each step in the synthesis process played a crucial role in the successful preparation of these novel peptides.

Biological Evaluation. The microorganisms, including *Escherichia coli* MTCC 443, *Pseudomonas aeruginosa* MTCC 1688, *Streptococcus pyogenes* MTCC 442, *Staphylococcus aureus* MTCC 96, *Aspergillus niger* MTCC 282, and *Candida albicans* MTCC 227, were obtained from King Abdullah University Hospital (KAUH), Irbid, Jordan. They were stored at $-70\text{ }^{\circ}\text{C}$ in trypticase-soy broth with 20% glycerol from BBL Microbiology Systems (Cockeysville, Maryland, USA) until they were required for batch susceptibility testing. To ensure purity and viability, the organisms were thawed and subcultured three times. The in vitro antimicrobial activities of the synthesized compounds 7a–i were studied using the conventional Mueller Hinton Broth-microdilution method.⁴⁶ This method is used for quantitative antimicrobial susceptibility testing and to determine the minimum inhibitory concentration (MIC) of antimicrobial agents. The test involved screening microorganisms for visible growth in broth consisting of different dilutions of the antimicrobial agents. The MIC value indicates the lowest concentration of an antimicrobial agent that inhibits visible growth within a specified time frame. The microbroth dilution method offers several advantages over the macrobroth dilution method, including miniaturization and automation through the use of disposable small plastic “microdilution” trays. Its practicality and popularity in research are attributed to advantages such as reproducibility, prepared panels, cost-effective reagents, and space optimization resulting from its miniaturization.^{47,48}

The Procedure for the Antibacterial Activity Assay. The strains employed in this study were recently acquired and stored under optimal conditions. The compounds underwent screening for their antibacterial activity in triplicate experiments against the bacteria, employing different concentrations of 1000, 500, 250, and 200 μM . Substances exhibiting effective

inhibition were subsequently subjected to dilution and further testing. The antibacterial assay employed the Mueller Hinton broth dilution method. A suspension of the respective bacteria at a concentration of 10 μM was inoculated on suitable media, and growth was monitored following incubation at $37\text{ }^{\circ}\text{C}$ for 1 to 2 days. The test mixture was intended to contain 10^8 cells/mL. Ampicillin served as the standard drug for assessing antibacterial activity in this study.⁴⁶

The Procedure for the Antifungal Activity Assay. The strains employed in this study were recently acquired and appropriately stored. The substances underwent screening for their antifungal properties in triplicate experiments against the fungi at varying concentrations of 1000, 500, 250, and 200 μM . The active compounds were further diluted and subjected to additional testing. The antifungal assay utilized the Muller Hinton broth dilution method. Fungal growth was monitored using Sabouraud’s dextrose broth at $28\text{ }^{\circ}\text{C}$ under aerobic conditions for a period of 48 h. Nystatin served as the standard for comparative analysis.⁴⁶

The antibacterial activities of novel THIQ dipeptide conjugate 7a–i against all the bacterial strains are shown in Table 1. The cationic peptide conjugate 7c, containing additional cationic AA His, was found to be 10 times more potent against *E. coli* and showed excellent activity with the highest MIC value of 33 μM among all the synthesized peptide conjugates as compared with the standard drug ampicillin, which had an MIC of 332 μM against the bacterial strain *E. coli*. Compound 7g with Ser showed excellent activity with an MIC value of 66 μM , five times more potent against *E. coli* as compared with standard ampicillin. THIQ dipeptide conjugates 7b, 7e, and 7h also exhibited good activities with MIC values of 166 μM and were two times more potent than the control drug. Other conjugates 7a, 7d, 7f, and 7i were slightly less active than the standard ampicillin against the bacterial strain *E. coli*. Against *P. aeruginosa*, 7e exhibited the highest activity among all the peptide derivatives with an MIC value of 83 μM , four times more potent as compared with the standard drug ampicillin, which had an MIC of 332 μM against the same. Moreover, compounds 7b and 7c also exhibited good activity with MIC values of 166 μM and were two times more potent than the control drug. The rest of the THIQ dipeptide conjugates were found to be less active, with MIC values of 332–664 μM , against *P. aeruginosa* as compared to the standard drug. Furthermore, among all the synthesized THIQ dipeptide conjugates, only 7c showed little antibacterial activity against *S. aureus* with an MIC value of 498 μM as compared to

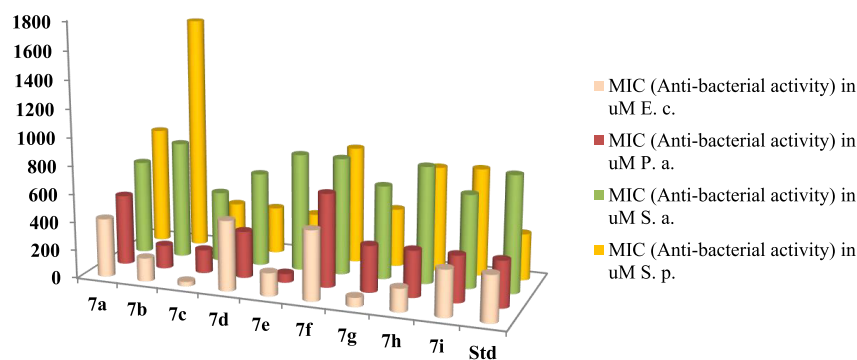


Figure 1. Antibacterial activity of title compounds 7a–i.

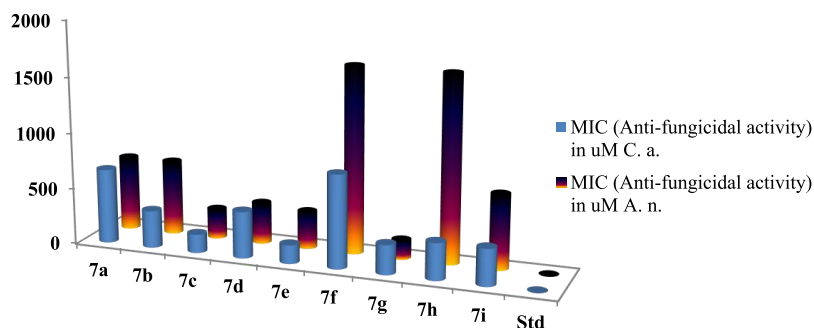


Figure 2. Antifungal activity of title compounds 7a–i.

the standard drug ampicillin (830 μM). The rest of the peptide derivatives did not show significant antibacterial activities, with MIC values of 664–830 μM , against *S. aureus* as compared to the standard drug. For the activity against *S. pyrogens*, only the derivative 7e showed very little activity with an MIC value of 315 μM , while the rest of the conjugates did not show significant activity as compared with a standard drug, which had an MIC of 332 μM (Figure 1). From the antibacterial activity study of all of the synthesized THIQ dipeptide conjugates, it was observed that compounds 7c and 7e with cationic AAs, His, and Arg, respectively, were the most active among all against the bacterial strains.

The antifungal activities of novel THIQ dipeptide conjugates 7a–i against all the fungal strains are shown in Table 1. Against *C. albicans*, conjugates 7c, 7e, and 7g were most active with MIC values of 166, 166, and 265 μM , respectively, compared to nystatin, which was active at 332 μM . Moreover, no significant activity was observed for the rest of the compounds against the fungal strain *C. albicans* as compared with the standard drug. 7c exhibited the highest activity when screened against the fungal strain *C. albicans* with an MIC value of 166 μM when compared to the standard drug nystatin with activity of 332 μM against the same. Its efficacy was twice that of the standard drug against *C. albicans*. Conjugates 7c and 7g also displayed good inhibition against *A. niger* with MIC values of 265 and 166 μM , respectively, as compared to the control drug. However, the rest of the synthesized derivatives showed less activity with MIC values in a range of 332–1661 μM against *A. niger* (Figure 2). After screening the THIQ dipeptide conjugates against all the desired microbial strains, it was observed that among all the conjugates 7c (His) and 7e (Arg), cationic peptide conjugates were the most active, which indicated the significance of the presence of cationic AAs in the peptide sequence for better activities, as mentioned earlier.

Molecular Docking Analysis. The molecular docking study was carried out using the glide module of the Schrodinger program. The crystal structure of *E. coli* DNA gyrase B was obtained from the Protein Data Bank using the PDB ID of 4KFG. The protein structure was optimized using the “protein preparation wizard” of the Schrodinger program, where hydrogens and missing side chains were added along with cap termination. The cocrystallized water molecules, which came along with crystal structures, were deleted. The protein structure was later optimized using the OPLS3 force field. Grid was generated by centralizing on the cocrystallized ligand present in the *E. coli* DNA gyrase B. At the same time, all the synthesized compounds were prepared and optimized using the LigPrep module of the Schrodinger program. The docking study of the synthesized peptides was carried out using the SP docking mode.^{49–51}

The significant antibacterial activity of the title compounds toward *E. coli* prompted us to conduct molecular docking simulations to better understand the ligand–protein interactions. As most of the synthesized peptides were showing significant antibacterial activity toward the *E. coli* and hence for the current study, we have selected the *E. coli* DNA gyrase as a target for the docking study. The protein structure of the *E. coli* DNA gyrase B was downloaded from the www.rcsb.org platform using the PDB ID of 4KFG. The details of the binding interaction and binding affinities against *E. coli* DNA gyrase B are mentioned in Table 2. The docking interactions of all the compounds 7a–i toward the *E. coli* DNA gyrase B enzyme are shown in Figures 3 and 4 and Figures S1–S7. Among the compounds examined for docking studies, 7b showed a high binding affinity with a low energy of (–6.708 kcal/mol) against 4KFG. Molecular docking data revealed that all the compounds show interaction networks with more than one amino acid in the receptor active pockets. The 2D and 3D interactions of top-scoring compound 7b are illustrated in

Table 2. Docking Score and Interacting Amino Acid Residues of the Synthesized Peptides

dock compounds	docking score (kcal/mol)	glide Emodel	glide Energy	interacting amino acid residues
compound 7b	-6.708	-85.903	-51.172	Asn-46, Asp-49, Glu-50, Arg-76
compound 7h	-6.592	-79.998	-52.68	Asn-46, Asp-49, Glu-50, Arg-76, Arg-136
compound 7g	-6.347	-80.344	-54.137	Asn-46, Asp-49, Glu-50, Arg-76
compound 7a	-6.455	-88.398	-53.805	Asn-46, Asp-49, Glu-50, Lys-110, Arg-76
compound 7d	-6.328	-78.13	-52.032	Arg-76, Lys-110, Asn-46, Asp-49, Glu-50
compound 7i	-6.005	-86.127	-54.887	Asn-46, Arg-76, Asp-49, Glu-50
compound 7f	-5.93	-75.532	-51.412	Asp-49, Glu-50, Lys-110, Arg-76
compound 7c	-5.92	-83.698	-53.326	Asn-46, Asp-49, Glu-50, Lys-110, Arg-76
compound 7e	-5.177	-77.565	-46.246	Asp-49, Lys-110, Arg-76, Asp-73

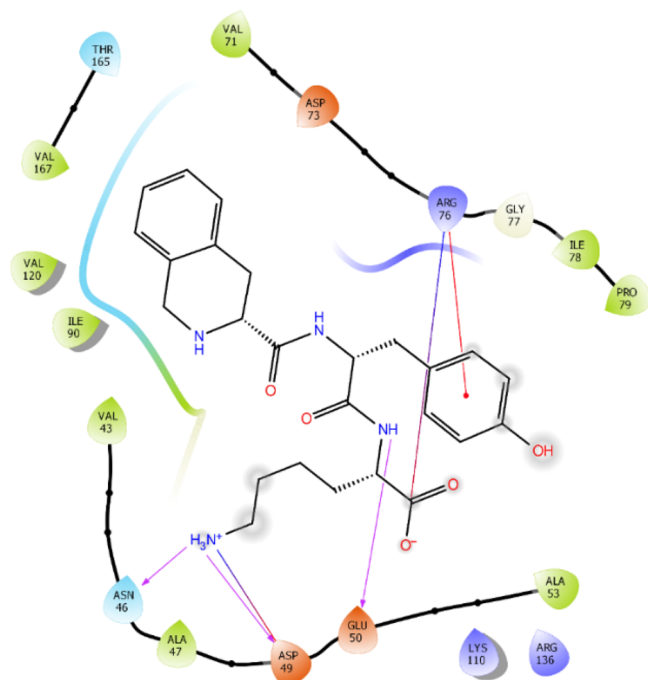
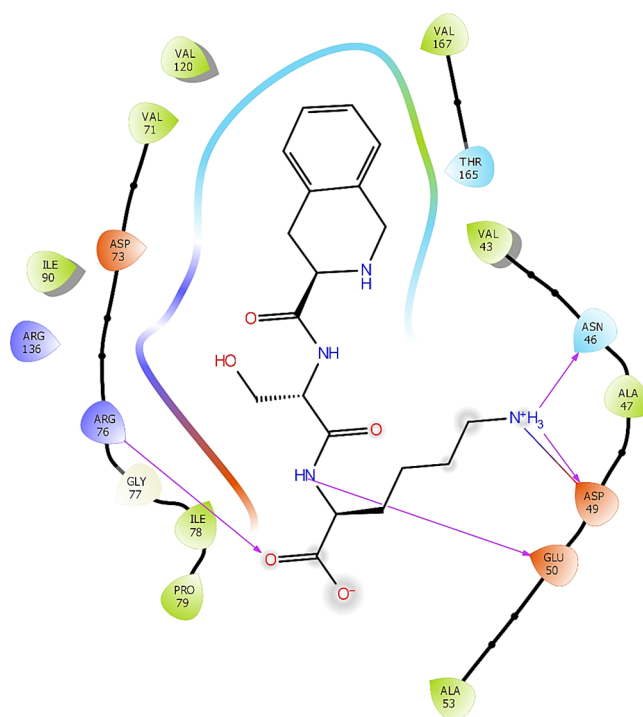
**Figure 3.** Docking interactions of compound 7b toward the *E. coli* DNA gyrase B enzyme.

Figure 3. Compound 7b established the π - π hydrophobic interaction and salt bridge with Arg-76 via the phenolic ring and ionized carboxylate ion. Glu-50 established the hydrogen bond interaction with the amidal NH group of compound 7b. The terminal quaternary amino group of compound 7b formed the salt bridge and hydrogen bond interaction with the Asp-49 amino acid and was involved in the hydrogen bond interaction with Asn-46. The results of the ligand-protein molecular docking provide valuable insight into the development of novel lead antibacterial materials that target the DNA gyrase enzyme of *E. coli*. Compound 7g established a hydrogen bond

**Figure 4.** Docking interactions of compound 7g toward the *E. coli* DNA gyrase B enzyme.

interaction with Glu-50 via the peptidal NH group and Arg-76 with the carbonyl oxygen of the terminal carboxylic acid group. Similarly, compound 7g formed the hydrogen bond interaction with Asn-46 and Asp-49 via the quaternized terminal amino group. The same quaternized terminal amino group also interacted with Asp-49 via the salt bridge interaction (Figure 4). The interacting amino acid residues of all of the synthesized peptides are given in Table 2.

Molecular Dynamics Simulation Study. The MD simulation was used to investigate the thermodynamic stability of the docked compound 7b-DNA gyrase B complex.^{52,53} The compound 7b-DNA gyrase B complex was solvated using the “single point charge (SPC)” water model. The system was neutralized by using Desmond’s system builder by adding seven Na⁺ counterions to an orthorhombic cell.^{54,55} The system was relaxed using a six-stage NPT protocol before the MD simulation.^{56,57} The compound 7b-DNA gyrase B complex was further submitted for a 100 ns MD simulation study. The stability of the complex was analyzed by evaluating the MD trajectories utilizing the “Desmond’s Simulation Interaction Diagram (SID)”.⁵³⁻⁵⁸

A molecular dynamics simulation was conducted for a duration of 100 ns to assess the durability of compound 7b within the DNA gyrase B cavity. To facilitate a 100 ns simulation, the docked complex was solvated in an explicit solvent within an orthorhombic box.^{53,54} The impact of compound 7b binding on the structural changes of *E. coli* DNA gyrase B was evaluated by analyzing the “root mean square deviation (RMSD) and root mean square fluctuation (RMSF)” over time.^{55,56} The observed fluctuations during the simulation can be utilized to gauge the stability of the protein in relation to its conformation. The protein structure is considered more stable when there are fewer variances or fluctuations. Figure 5 displays the RMSD graph of the C α atoms of *E. coli* DNA gyrase B over a duration of 100 ns. The compound 7b-*E. coli*

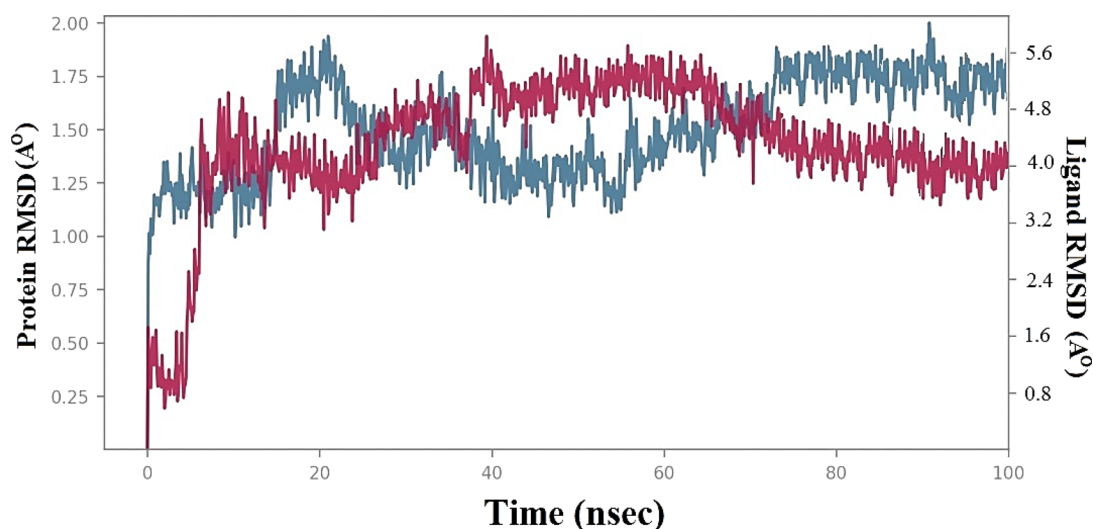


Figure 5. RMSD of ligand **7b** with respect to the protein DNA gyrase B.

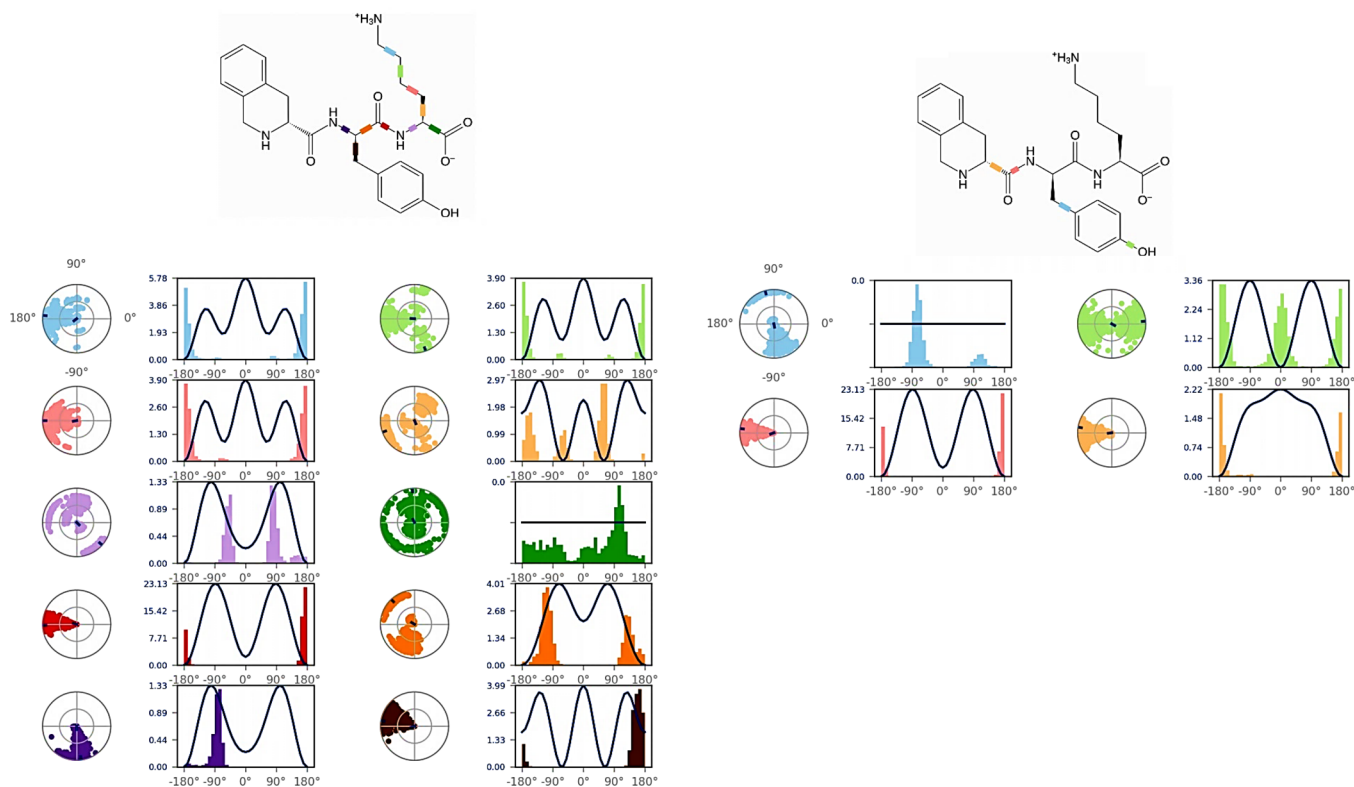


Figure 6. Ligand (compound **7b**) torsion profile during the 100 ns time of simulation.

DNA gyrase B complex remained in the equilibration state until the 6 ns time of the simulation with ligand RMSD of 3.6 Å. From 6.20 to 13 ns time of the simulation, slightly higher fluctuation of the ligand was observed with RMSD of 3.69–4.09 Å due to initial equilibration of the system. Compound **7b** achieved stability from 14.90 to 26.80 ns time of the simulation. The higher RMSD (5.27–5.24 Å) of compound **7b** was observed from 37.50 to 70.80 ns time of simulation due to the presence of a rotatable peptide bond in compound **7b** (Figure 6). The ligand–torsion profile in Figure 6 indicates that the peptide backbone of compound **7b** is highly fluctuable during 100 ns of the simulation. From 72 ns onward, the ligand

was stabilized inside the pocket of the *E. coli* DNA gyrase B with RMSD of 4.5 Å.

The flexibility of *E. coli* DNA gyrase C α atoms was assessed by calculating the RMSF values, which provided insights into the impact of compound **7b** on their flexibility.^{57,58} During the simulation, compound **7b** interacted with 33 amino acids of *E. coli* DNA gyrase protein including Glu-42, Val-43, Asp-45, Asn-46, Ala-47, Asp-49, Glu-50, Ala-53, Val-71, Asp-73m Arg-76, Gly-77, Ile-78, Pro-79, Ile-82, Ala-86, Ile-90, Val-93, Leu-94, Lys-110, Val-111, Gly-113, Gly-114, Leu-115, His-116, Gly-117, Gly-119, Val-120, Ser-121, Arg-130, Thr-165, Val-167, and Asn-178. All of these interactions are indicated by vertical bars colored green, as shown in Figure 7. The RMSF

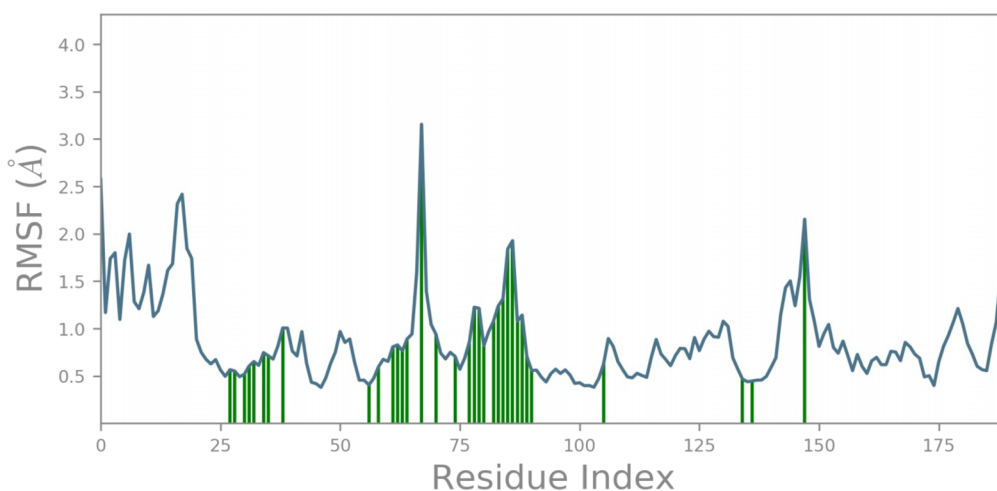


Figure 7. RMSF of DNA gyrase B during the 100 ns time of simulation, where the green line indicates the interaction of residues with the ligand (compound 7b).

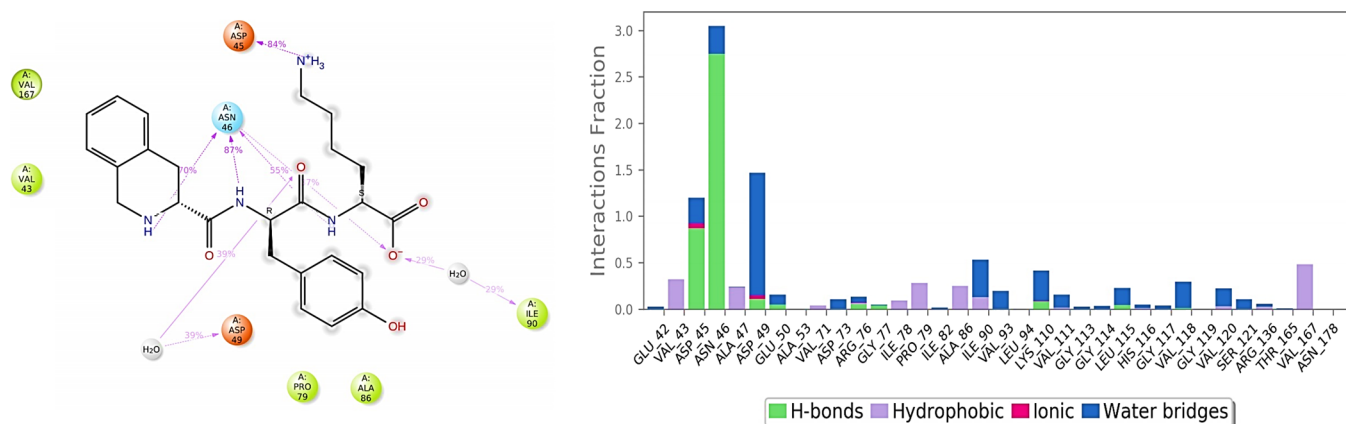


Figure 8. 2D interaction diagram of compound 7b and protein–ligand interaction analysis of the MD trajectory.

graph suggests that the fluctuation in the *E. coli* DNA gyrase C α atoms is minimum within the RMSF with the value of 2 Å when in complex with compound 7b, except for the amino acid Ile-82, where RMSF reached 3.15 Å. Overall, these results suggest that compound 7b made the protein–ligand complex more stable during the 100 ns MD simulation.

Figure 8 shows a protein–ligand contact analysis during MD simulations. It was observed that Asn-46 formed a prominent hydrogen bond interaction with the NH of the isoquinoline ring (70%) and two different NH (87 and 55%) of the peptide backbone. Asp-45 also established the hydrogen bond interaction (84%) with the terminal quaternized amino group of the peptide backbone. Apart from it, water-mediated hydrogen bonding was seen with Asp-49 and Ile-90. Hydrophobic interaction of the isoquinoline and phenol ring was observed with the Val-167, Val-43, Pro-79, and Ala-86 amino acid residues.

MATERIALS AND METHODS

The 2-chlorotrityl chloride (2-CTC) resin was utilized for the synthesis of a series of short peptide derivatives with a THIQ-3-carboxylic acid constituent. Highly efficient loading estimation is obtained by using such resin. This resin is mainly used for the synthesis of short-chain peptides.⁵⁸ It was purchased from Merck. Fmoc(9-fluorenylmethoxycarbonyl)-protected L-amino acids were utilized and acquired from Sichuan, China.

HBTU (2-(1*H*-benzotriazol-1-yl)-1,1,3,3-tetramethyluronium) and triisopropylsilane (TIS) were acquired from a survival chemical. HOBt-H₂O (*N*-hydroxybenzotriazole monohydrate), diisopropylethylamine (DIPEA), and trifluoroacetic acid (TFA) were acquired from Spectrochem. Phenol was acquired from SD Fine Chemicals. A fully automated CSBio peptide synthesizer (CS136X) was utilized for the synthesis of derivatives.³¹

An open capillary method was utilized to determine the melting points that were uncorrected. The Kaiser test was used for monitoring the deprotection and condensation reactions. A mixture of ethyl acetate and *n*-hexanes was used for the purification of the derivatives. A Shimadzu liquid chromatography mass spectrometry (LC-MS) (at 70 eV) mass spectrometer (ESI) was used to determine the mass spectra. A Bruker Avance 400 MHz NMR (nuclear magnetic resonance) spectrometer was used to determine the ¹H and ¹³C NMR spectra using DMSO-*d*₆ (deuterated dimethyl sulfoxide) solvent.³¹

EXPERIMENTAL SECTION

Synthetic Route for the Formation of Intermediate 1.

The 2-CTC resin was introduced into the peptide synthesizer with a substitution of 1.0 mmol/g. The resin was initially rinsed with dichloromethane (DCM; 10 vol) and then drained. After that, DCM (10 volumes) was added and the reaction

mass was stirred for 60 min for swelling before being drained. Following this, Fmoc-Lys(Boc)-OH (3.0 equiv) was dissolved in DCM (eight volumes) and transferred to the reaction vessel. DIPEA (6 equiv) was subsequently added to the reaction vessel and stirred at 25 °C for 2 h. The peptidyl resin was filtered after the 2 h mark and washed twice with DCM and once with dimethylformamide (DMF).⁵⁹ A solution containing DIPEA, methanol (MeOH), and DCM (1:2:7) was used to cap the unreacted functional groups of the resin. The loading percentage was monitored using an ultraviolet (UV) spectrophotometer.³¹

Synthetic Route for the Formation of Intermediates

6a–i. The standard Fmoc/*t*-Bu(*t*-butyl)/Boc(*t*-butyloxycarbonyl) protocol was employed to produce the desired intermediates **6a–i** through the solid-phase peptide synthesis (SPPS) method. In the SPPS reaction vessel, the Fmoc-Lys(Boc)-2-CTC resin was swollen in 20 volumes of DMF for 30 min. The CSBio peptide synthesizer facilitated the synthesis of the intended intermediates. Postswelling, the following steps were repeated for the synthesis of the intermediates: (a) deprotection of the Fmoc group was carried out using 20% piperidine/DMF (v/v) (10 (v)). The resin was washed twice (5 and 10 min each). The Kaiser test was used to ensure complete deprotection, indicated by the appearance of a blue color. Subsequently, the reaction mass (peptidyl resin) was filtered and washed three times with DMF, once with isopropyl alcohol (IPA), and three times again with DMF. (b) For all the condensation reactions, Fmoc amino acid/Fmoc-D-Tic-OH (3.0 equiv, 3 mmol concerning initial resin loading), HBTU (3.0 equiv, 3 mmol), HOBt·H₂O (3.0 equiv, 3 mmol), and DIPEA (6.0 equiv, 6 mmol) in eight volumes of DMF were utilized. All the condensation reactions required 1 h of stirring. The Kaiser test was used to confirm the completion of the reaction, indicated by a colorless test solution and beads. The reaction mass (peptidyl resin) was then filtered and washed five times with DMF to yield **5a–i**.⁶⁰ Additionally, group deprotection of **5a–i** was carried out using 20% piperidine/DMF (v/v) (10 (v)) to obtain the desired Fmoc intermediates **6a–i**. The Kaiser test was used to confirm the deprotection of the Fmoc group, where blue-color resin beads and solution were observed, confirming the completion of the step. Following this, the reaction mass (peptidyl resin) was filtered and washed five times with DMF to produce **6a–i**.³¹

Synthetic Route for the Synthesis of Desired THIQ Dipeptide Derivatives 7a–i. A cleavage cocktail consisting of a mixture of TFA:TIS:H₂O (80:10:10) (10 mL/g) was utilized for the cleavage of the side chain and CTC resin.⁶¹ The protected peptidyl resin was stirred in the cleavage cocktail for 3 h at 27 ± 2 °C. After this duration, the reaction mass was filtered and the filtrate obtained was precipitated using chilled diisopropyl ether (DIPE) (50 (v)). Subsequently, the reaction mass was stirred at 0–5 °C for 2 h, filtered, and washed thrice with chilled DIPE (10 (v)). Finally, the wet cake was dried at 30 °C under vacuum to yield the desired products.³¹

CONCLUSIONS

THIQ is a privileged scaffold present in many clinically used drug molecules. In this article, we demonstrated a new series of THIQ conjugates with dipeptide derivatives synthesized using a solid-phase peptide synthetic technique. The synthesized THIQ conjugates were characterized using ¹H NMR, ¹³C, and mass spectrometric analysis techniques. The synthesized

THIQ dipeptide analogues were evaluated for their antimicrobial activities. The analysis found that the conjugates exhibited significant antibacterial and antifungal activity as compared to standard drugs, ampicillin and nystatin, respectively. Especially, the cationic THIQ dipeptide conjugates **7c** and **7e** showed significant activities against all the screened microbial strains due to the presence of additional cationic AA, His and Arg, respectively. All the synthesized derivatives were subjected for molecular docking studies to investigate their intermolecular interaction networks and binding affinities toward the *E. coli* DNA gyrase enzyme. Among the synthesized compounds, compound **7b** displayed significant docking. Furthermore, the MD simulation study at 100 ns time reflects that compound **7b** was stable inside the cavity of the *E. coli* DNA gyrase. The structural and functional insights from experimental, biological, and computational studies conducted on DNA gyrase assembly with synthesized THIQ derivatives shed a light on further development and potential of antimicrobials using hybrid heterocycles with peptides.

ASSOCIATED CONTENT

Supporting Information

The Supporting Information is available free of charge at <https://pubs.acs.org/doi/10.1021/acsomega.3c05961>.

¹H and ¹³C NMR, and mass spectral data (PDF)

AUTHOR INFORMATION

Corresponding Authors

Ghazala Muteeb – Department of Nursing, College of Applied Medical Science, King Faisal University, Al-Ahsa 31982, Saudi Arabia; orcid.org/0000-0002-3328-3559; Email: graza@kfu.edu.sa

Enrique Delgado-Alvarado – Micro and Nanotechnology Research Center and Facultad de Ciencias Químicas, Universidad Veracruzana, Boca del Río 94294, Mexico; orcid.org/0000-0002-6354-5222; Email: endelgado@uv.mx

Yashwantsinh Jadeja – Department of Chemistry, Marwadi University, Rajkot, Gujarat 360003, India; orcid.org/0000-0002-6072-0654; Email: drysjadeja@gmail.com

Authors

Sunil R. Tivari – Department of Chemistry, Marwadi University, Rajkot, Gujarat 360003, India

Siddhant V. Kokate – Department of Chemistry, S.S.C. College, Junnar, Pune, Maharashtra 410502, India

José L. Belmonte-Vázquez – Facultad de Química, Universidad Nacional Autónoma de México, Ciudad de México 04510, Mexico

Tushar Janardan Pawar – Red de Estudios Moleculares Avanzados, Clúster Científico y Tecnológico BioMimic del Instituto de Ecología, Xalapa, Veracruz 91073, Mexico

Harun Patel – Department of Pharmaceutical Chemistry, R. C. Patel Institute of Pharmaceutical Education and Research, Dhule, Maharashtra 425405, India; orcid.org/0000-0003-0920-1266

Iqrar Ahmad – Department of Pharmaceutical Chemistry, R. C. Patel Institute of Pharmaceutical Education and Research, Dhule, Maharashtra 425405, India

Manoj S. Gayke – Department of Chemistry, School of Science, Indrashil University, Mehsana, Gujarat 382715, India

Rajesh S. Bhosale – Department of Chemistry, School of Science, Indrashil University, Mehsana, Gujarat 382715, India

Vicky D. Jain – Department of Chemistry, Marwadi University, Rajkot, Gujarat 360003, India; orcid.org/0000-0001-5682-8913

Complete contact information is available at:
<https://pubs.acs.org/10.1021/acsomega.3c05961>

Author Contributions

[†]Both authors have equal contributions.

Funding

This work was supported by the Deanship of Scientific Research, Vice Presidency for Graduate Studies and Scientific Research, King Faisal University, Saudi Arabia [Grant No. 5213].

Notes

The authors declare no competing financial interest. All the authors are responsible for the following: study conception and design, data collection, analysis, interpretation of results, and manuscript preparation. All the authors reviewed the results and approved the final version of the manuscript.

ACKNOWLEDGMENTS

The authors are thankful to the Deanship of Scientific Research, Vice Presidency for Graduate Studies and Scientific Research, King Faisal University, Saudi Arabia, for the financial support. The authors also thank University Grants Commission, New Delhi, and Marwadi University for the technical and academic support.

REFERENCES

- (1) World Health Organization. *Global antimicrobial resistance surveillance system (GLASS) report: Early implementation 2016–2017*, World Health Organization 2019.
- (2) Singer, A. C.; Shaw, H.; Rhodes, V.; Hart, A. Review of Antimicrobial Resistance in the Environment and Its Relevance to Environmental Regulators. *Front. Microbiol.* **2016**, *7*, 1728.
- (3) Marshall, B. M.; Levy, S. B. Food animals and antimicrobials: impacts on human health. *Clin. Microbiol. Rev.* **2011**, *24*, 718–733.
- (4) Ventola, C. L. The antibiotic resistance crisis: part 1: causes and threats. *Pharm. Ther.* **2015**, *277*.
- (5) O'Neill, J. Tackling drug-resistant infections globally: Final report and recommendations; Analysis & Policy Observatory, 2016.
- (6) Hancock, R.; Sahl, H. G. Antimicrobial and host-defense peptides as new anti-infective therapeutic strategies. *Nat. Biotechnol.* **2006**, *24*, 1551–1557.
- (7) Mahlapuu, M.; Håkansson, J.; Ringstad, L.; Björn, C. Antimicrobial Peptides: An Emerging Category of Therapeutic Agents. *Front. Cell. Infect. Microbiol.* **2016**, *6*, 194.
- (8) Sharma, K. K.; Ravi, R.; Maurya, I. K.; Kapadia, A.; Khan, S. I.; Kumar, V.; Tikoo, K.; Jain, R. Modified histidine containing amphipathic ultrashort antifungal peptide, His[2-p-(n-butyl)phenyl]-Trp-Arg-OMe exhibits potent anticryptococcal activity. *Eur. J. Med. Chem.* **2021**, *223*, 113635–113650.
- (9) Sharma, K. K.; Maurya, I. K.; Khan, S. I.; Jacob, M. R.; Kumar, V.; Tikoo, K.; Jain, R. Discovery of a membrane-active, ring-modified histidine containing ultrashort amphiphilic peptide that exhibits potent inhibition of *Cryptococcus neoformans*. *J. Med. Chem.* **2017**, *60*, 6607–6621.
- (10) Tivari, S. R.; Kokate, S. V.; Sobhia, E. M.; Kumar, S. G.; Shelar, U. B.; Jadeja, Y. S. A Series of Novel Bioactive Cyclic Peptides: Synthesis by Head-to-Tail Cyclization Approach, Antimicrobial

Activity and Molecular Docking Studies. *ChemistrySelect* **2022**, *7*, No. e202201481.

(11) Mant, C. T.; Jiang, Z.; Gera, L.; Davis, T.; Nelson, K. L.; Bevers, S.; Hodges, R. S. Novo Designed Amphipathic α -Helical Antimicrobial Peptides Incorporating Dab and Dap Residues on the Polar Face to Treat the Gram-Negative Pathogen, *Acinetobacter baumannii*. *J. Med. Chem.* **2019**, *67*, 3354–3366.

(12) Mookherjee, N.; Anderson, M. A.; Haagsman, H. P.; Davidson, D. J. Antimicrobial host defence peptides: functions and clinical potential. *Nat. Rev. Drug Discovery* **2020**, *19*, 311–332.

(13) Mishra, B.; Reiling, S.; Zarena, D.; Wang, G. Host defense antimicrobial peptides as antibiotics: design and application strategies. *Curr. Opin. Chem. Biol.* **2017**, *38*, 87–96.

(14) Lāce, I.; Cotroneo, E. R.; Hesselbarth, N.; Simeth, N. A. Artificial peptides to induce membrane denaturation and disruption and modulate membrane composition and fusion. *J. Peptide Sci.* **2023**, *29*, No. e3466.

(15) An, C.; Wei, S.; Dao, Y.; Wang, X.; Dong, W.; You, X.; Tian, C.; Zhang, Z.; Dong, S. Discovery of endosomal cell-penetrating peptides based on bacterial membrane-targeting sequences. *Bioorg. Chem.* **2023**, *134*, No. 106424.

(16) Steckbeck, J. D.; Deslouches, B.; Montelaro, R. C. Antimicrobial peptides: new drugs for bad bugs? *Expert Opin. Biol. Ther.* **2014**, *14*, 11–14.

(17) Hewitt, W. M.; Leung, S. S.; Pye, C. R.; Ponkey, A. R.; Bednarek, M.; Jacobson, M. P.; Lokey, R. S. Cell-permeable cyclic peptides from synthetic libraries inspired by natural products. *J. Am. Chem. Soc.* **2015**, *137*, 715–721.

(18) Tivari, S.; V Kokate, S.; B Shelar, U.; Jadeja, Y. The design, synthesis and biological evaluation of the peptide derivatives containing guanidine moiety with 5-chloro-thiophene-2-carboxylic acid conjugates. *RASAYAN J. Chem.* **2022**, *15*, 875–884.

(19) Tivari, S. R.; Kokate, S. V.; Gayke, M. S.; Ahmad, I.; Patel, H.; Kumar, S. G.; Jadeja, Y. S. A Series of dipeptide Derivatives Containing (S)-5-Oxo-pyrrolidine-2-carboxylic acid Conjugates: Design, Solid-Phase Peptide Synthesis, *in vitro* Biological Evaluation, and Molecular Docking Studies. *ChemistrySelect* **2022**, *7*, No. e202203462.

(20) Wu, G.; Ding, J. Antimicrobial peptides: Promising alternatives in the post-antibiotic era. *Med. Res. Rev.* **2021**, *831* DOI: [10.1002/med.21542](https://doi.org/10.1002/med.21542).

(21) Chen, Y.; Guarnieri, M. T.; Vasil, A. I.; Vasil, M. L.; Mant, C. T.; Hodges, R. S. Role of peptide hydrophobicity in the mechanism of action of alpha-helical antimicrobial peptides. *Antimicrob. Agents Chemother.* **2007**, *51*, 1398–406.

(22) Shi, S.; Nguyen, P. K.; Cabral, H. J.; Diez-Barroso, R.; Derry, P. J.; Kanahara, S. M.; Kumar, V. A. Development of peptide inhibitors of HIV transmission. *Bioact Mater.* **2016**, *1*, 109–121.

(23) Wibowo, D.; Zhao, C.-X. Recent achievements and perspectives for large-scale recombinant production of antimicrobial peptides. *Appl. Microbiol. Biotechnol.* **2019**, *103*, 659–671.

(24) Grubor, B.; Meyerholz, D. K.; Ackermann, M. R. Collectins and cationic antimicrobial peptides of the respiratory epithelia. *Veterinary Pathology* **2006**, *43*, 595–612.

(25) Hemshekhar, M.; Choi, K. Y. G.; Mookherjee, N. Host Defense Peptide LL-37-Mediated Chemoattractant Properties, but Not Anti-Inflammatory Cytokine IL-1RA Production, Is Selectively Controlled by Cdc42 Rho GTPase via G Protein-Coupled Receptors and JNK Mitogen-Activated Protein Kinase. *Front. Immunol.* **2018**, *9*, 1871.

(26) Bahar, A. A.; Ren, D. Antimicrobial Peptides. *Pharmaceuticals* **2013**, *6*, 1543–1575.

(27) Mabkhot, Y. N.; Alatibi, F.; El-Sayed, N. N. E.; Al-Showiman, S.; Kheder, N. A.; Wadood, A.; Rauf, A.; Bawazeer, S.; Hadda, T. B. Antimicrobial Activity of Some Novel Armed Thiophene Derivatives and Petra/Osiris/Molinspiration (POM) Analyses. *Molecules* **2016**, *21*, 222.

(28) Perry, N. B.; Blunt, J. W.; Munro, M. H. Cytotoxic pigments from New Zealand sponges of the genus *Latrunculia*: discorhabdins A, B, and C. *Tetrahedron* **1988**, *44*, 1727–1734.

- (29) Kobayashi, J. I.; Cheng, J. F.; Ishibashi, M.; Nakamura, H.; Ohizumi, Y.; Hirata, Y.; Sasaki, T.; Lu, H.; Clardy, J. Prianosin A, a novel antileukemic alkaloid from the Okinawan marine sponge Prianos melanos. *Tetrahedron Lett.* **1987**, *28*, 4939–4942.
- (30) Al-Smadi, M.; Al-Momani, F. Synthesis, Characterization and Antimicrobial Activity of New 1,2,3-Selenadiazoles. *Molecules* **2008**, *13*, 2740–2749.
- (31) Tivari, S. R.; Kokate, S. V.; Delgado-Alvarado, E.; Gayke, M. S.; Kotmale, A.; Patel, H.; Ahmad, I.; Sobhia, E. M.; Kumar, S. G.; Lara, B. G.; Jain, V. D.; Jadeja, Y. A novel series of dipeptide derivatives containing indole-3-carboxylic acid conjugates as potential antimicrobial agents: the design, solid phase peptide synthesis, *in vitro* biological evaluation, and molecular docking study. *RSC Adv.* **2023**, *13*, 24250–24263.
- (32) Raimondi, M. V.; Presentato, A.; Li Petri, G.; Buttacavoli, M.; Ribaud, A.; De Caro, V.; Alduina, R.; Cancemi, P. New Synthetic Nitro-Pyrrolomycins as Promising Antibacterial and Anticancer Agents. *Antibiotics* **2020**, *9*, 292.
- (33) Raimondi, M. V.; Listro, R.; Cusimano, M. G.; la Franca, M.; Faddetta, T.; Gallo, G.; Schillaci, D.; Collina, S.; Leonchiks, A.; Barone, G. Pyrrolomycins as antimicrobial agents. Microwave-assisted organic synthesis and insights into their antimicrobial mechanism of action. *Bioorg. Med. Chem.* **2019**, *27*, 721–728.
- (34) Spanò, V.; Rocca, R.; Barreca, M.; Giallombardo, D.; Montalbano, A.; Carbone, A.; Raimondi, M. V.; Gaudio, E.; Bortolozzi, R.; Bai, R.; Tassone, P.; Alcaro, S.; Hamel, E.; Viola, G.; Bertoni, F.; Barraja, P. Pyrrolo[2',3':3,4]cyclohepta[1,2-d][1,2]-oxazoles, a New Class of Antimitotic Agents Active against Multiple Malignant Cell Types. *J. Med. Chem.* **2020**, *63*, 12023–12042.
- (35) Yang, C.; Fang, Y.; Hu, Y.; Tian, T.; Liao, G. Discovery of new tetrahydroisoquinolines as potent and selective LSD1 inhibitors for the treatment of MLL-rearranged leukemia. *Eur. J. of Med. Chem.* **2023**, *257*, No. 115516.
- (36) Fayez, S.; Feineis, D.; Ake Assi, L.; Kaiser, M.; Brun, R.; Awale, S.; Bringmann, G. Ancistrobrevines E-J and related naphthylisoquinoline alkaloids from the West African liana *Ancistrocladus abbreviatus* with inhibitory activities against *Plasmodium falciparum* and PANC-1 human pancreatic cancer cells. *Fitoterapia* **2018**, *131*, 245–259.
- (37) Lu, G. L.; Tong, A. S. T.; Conole, D.; Sutherland, H. S.; Choi, P. J.; Franzblau, S. G.; Upton, A. M.; Lotlikar, M. U.; Cooper, C. B.; Denny, W. A.; Palmer, B. D. Synthesis and structure-activity relationships for tetrahydroisoquinoline-based inhibitors of *Mycobacterium tuberculosis*. *Bioorg. Med. Chem.* **2020**, *28*, No. 115784.
- (38) Xu, H.; Lu, X.; Sun, T.; He, Q.; Qi, Y.; Lin, Y.; Yang, X.; Zhang, L.; Ling, Y.; Zhang, X. Novel 1,2,3,4-tetrahydroisoquinoline-based Schiff bases as laccase inhibitors: Synthesis and biological activity, 3D-QSAR, and molecular docking studies. *J. Mol. Struct.* **2023**, *1285*, No. 135526.
- (39) Gabet, B.; Kuo, P. C.; Fuentes, S.; Patel, Y.; Adow, A.; Alsakka, M.; Avila, P.; Beam, T.; Yen, J. H.; Brown, D. A. Identification of N-benzyl tetrahydroisoquinolines as novel anti-neuroinflammatory agents. *Bioorg. Med. Chem.* **2018**, *26*, 5711–5717.
- (40) George, A.; Gopi Krishna Reddy, A.; Satyanarayana, G.; Raghavendra, N. K. 1,2,3,4-Tetrahydroisoquinolines as inhibitors of HIV-1 integrase and human LEDGF/p75 interaction. *Chem. Biol. Drug Des.* **2018**, *91*, 1133–1140.
- (41) Barkhordarian, M.; Lawrence, J. A.; Ulsan, S.; Erbay, M. I.; Aronow, W. S.; Gupta, R. Benefit and risk evaluation of Quinapril hydrochloride. *Expert Opin. Drug Saf.* **2023**, *22* (4), 271–277.
- (42) Pragyandipta, P.; Pedapati, R. K.; Reddy, P. K.; Nayek, A.; Meher, R. K.; Guru, S. K.; Kantavari, S.; Naik, P. K. Rational design of novel microtubule targeting anticancer drugs N-imidazopyridine noscapinoids: Chemical synthesis and experimental evaluation based on *in vitro* using breast cancer cells and *in vivo* using xenograft mice model. *Chem.-Biol. Interact.* **2023**, *382*, No. 110606.
- (43) Bamel, K.; Mondal, N. *In vitro* culture using nicotine and d-tubocurarine and *in silico* analysis depict the presence of acetylcholine receptor (AChR) in tomato (*Solanum lycopersicum* L.). *Vitro Cell. Dev. Biol.-Plant* **2023**, *59*, 39–48.
- (44) Preetam, S.; Jonnalagadda, S.; Kumar, L.; Rath, R.; Chattopadhyay, S.; Alghamdi, B. S.; Abuzenadah, A. M.; Jha, N. K.; Gautam, A.; Malik, S.; Ashraf, G. M. Therapeutic potential of lipid nanosystems for the treatment of Parkinson's disease. *Ageing Res. Rev.* **2023**, *89*, No. 101965.
- (45) Palomo, J. M. Solid-phase peptide synthesis: an overview focused on the preparation of biologically relevant peptides. *RSC Adv.* **2014**, *4*, 32658–32672.
- (46) Desai, N. C.; Jadeja, K. A.; Jadeja, D. J.; Khedkar, V. M.; Jha, P. C. Design, synthesis, antimicrobial evaluation, and molecular docking study of some 4-thiazolidinone derivatives containing pyridine and quinazoline moiety. *Synth. Commun.* **2020**, *51*, 1–963.
- (47) Kowalska-Krochmal, B.; Dudek-Wicher, R. The Minimum Inhibitory Concentration of Antibiotics: Methods, Interpretation. *Clinical Relevance. Pathogens* **2021**, *10*, 165.
- (48) Jorgensen, J. H.; Ferraro, M. J. Antimicrobial susceptibility testing: a review of general principles and contemporary practices. *Clin. Infect. Dis.* **2009**, *49*, 1749–1755.
- (49) Patel, H. M.; Palkar, M.; Karpoomath, R. Exploring MDR-TB Inhibitory Potential of 4-Aminoquinazolines as *Mycobacterium tuberculosis* N-Acetylglucosamine-1-Phosphate Uridyltransferase (GlmUTMB) Inhibitors. *Chem. Biodivers.* **2020**, *17*, No. e2000237.
- (50) Agwupuyeh, J. A.; Louis, H.; Gber, T. E.; Ahmad, I.; Agwamba, E. C.; Samuel, A. B.; Ejiako, E. J.; Patel, H.; Ita, I. T.; Basse, V. M. Molecular modeling and DFT studies of diazenylphenyl derivatives as a potential HBV and HCV antiviral agents. *Chem. Phys. Impact* **2022**, *5*, No. 100122.
- (51) Alagumuthu, M.; Muralidharan, V. P.; Andrew, M.; Ahmed, M. H.; Iyer, S. K.; Arumugam, S. Computational Approaches to Develop Isoquinoline Based Antibiotics through DNA gyrase Inhibition Mechanisms Unveiled through Antibacterial Evaluation and Molecular Docking. *Mol. Informatics* **2018**, *37*, No. e1800048.
- (52) Ahmad, I.; Jadhav, H.; Shinde, Y.; Jagtap, V.; Girase, R.; Patel, H. Optimizing Bedaquiline for cardiotoxicity by structure based virtual screening, DFT analysis and molecular dynamic simulation studies to identify selective MDR-TB inhibitors. *In Silico Pharmacol.* **2021**, *9*, 1–5.
- (53) Pawara, R.; Ahmad, I.; Nayak, D.; Wagh, S.; Wadkar, A.; Ansari, A.; Belamkar, S.; Surana, S.; Nath Kundu, C.; Patil, C.; Patel, H. Novel, selective acrylamide linked quinazolines for the treatment of double mutant EGFR-L858R/T790M Non-Small-Cell lung cancer (NSCLC). *Bioorg. Chem.* **2021**, *115*, No. 105234.
- (54) Pandey, R.; Dubey, I.; Ahmad, I.; Mahapatra, D. K.; Patel, H.; Kumar, P. *In silico* Study of Some Dexamethasone Analogs and Derivatives against SARS-CoV-2 Target: A Cost-effective Alternative to Remdesivir for Various COVID Phases. *Curr. Chin. Sci.* **2022**, *2*, 294–309.
- (55) Ayipo, Y. O.; Ahmad, I.; Najib, Y. S.; Sheu, S. K.; Patel, H.; Mordi, M. N. Molecular modelling and structure-activity relationship of a natural derivative of o-hydroxybenzoate as a potent inhibitor of dual NSP3 and NSP12 of SARS-CoV-2: *In silico* study. *J. Biomol. Struct. Dyn.* **2022**, 1959–7.
- (56) Ghosh, A.; Sarmah, P.; Patel, H.; Mukerjee, N.; Mishra, R.; Alkahtani, S.; Varma, R. S.; Baishya, D. Nonlinear molecular dynamics of quercetin in *Gynocardia odorata* and *Diospyros malabarica* fruits: Its mechanistic role in hepatoprotection. *PLoS One* **2022**, *17*, No. e0263917.
- (57) Hammouda, M. B.; Ahmad, I.; Hamdi, A.; Dbeibia, A.; Patel, H.; Bouali, N.; Hamadou, W. S.; Hosni, K.; Ghannay, S.; Alminderej, F.; Noumi, E.; Snoussi, M.; Aouadi, K.; Kadri, A. Design, synthesis, biological evaluation and *in silico* studies of novel 1,2,3-triazole linked benzoxazine-2,4-dione conjugates as potent antimicrobial, antioxidant and anti-inflammatory agents. *Arab. J. Chem.* **2022**, *15*, No. 104226.
- (58) Jaradat, D. M. M. Thirteen decades of peptide synthesis: key developments in solid phase peptide synthesis and amide bond formation utilized in peptide ligation. *Amino Acids* **2018**, *50*, 39–68.
- (59) Made, V.; Els-Heindl, S.; Beck-Sickinger, A. G. Automated solid-phase peptide synthesis to obtain therapeutic peptides. *Beilstein J. Org. Chem.* **2014**, *10*, 1197–1212.

(60) Kaiser, E.; Colescott, R. L.; Bossinger, C. D.; Cook, P. I. Color test for detection of free terminal amino groups in the solid-phase synthesis of peptides. *Anal. Biochem.* **1970**, *34*, 595–598.

(61) Behrendt, R.; White, P.; Offer, J. Advances in Fmoc solid-phase peptide synthesis. *J. Pept. Sci.* **2016**, *22*, 4–27.